

# INFLUENCE OF DOPANT SPECIES ON ELECTRON MOBILITY IN HEAVILY DOPED SEMICONDUCTORS

G. Kaiblinger-Grujin, H. Kosina, Ch. Köpf, and S. Selberherr

Institute for Microelectronics, TU Vienna  
Gusshausstrasse 27-29  
A-1040 Vienna, Austria

**Keywords :** electron mobility, ionized impurity scattering, Thomas-Fermi atomic model

## Abstract

We present a new theoretical approach to study the influence of the dopant species on the electron drift mobility in doped semiconductors under low electric fields. The charge distribution of the impurities is described by the Thomas-Fermi theory in the energy functional formulation. We have included many-particle effects, such as dispersive screening and multiple scattering, which become important in heavily doped semiconductors. Analytical expressions for the scattering cross section for various species of dopants using the Born approximation up to second order are derived. Monte Carlo simulations including all important scattering mechanism have been performed for Si, GaAs, and InP in the doping concentration range of  $10^{15}$  to  $10^{21}$   $\text{cm}^{-3}$ . The dependence on donor species is significant for concentrations beyond  $10^{18}$   $\text{cm}^{-3}$ , whereas the minority electron mobility is not affected by different dopants. Not only confirm the results the experimental data of the mobility enhancement of minority electrons compared to majority electrons in degenerated semiconductors but also the lower electron mobility in As-doped Si in comparison to P-doped Si.

## Introduction

As semiconductor device dimensions decreasingly approach  $0.1 \mu\text{m}$ , it becomes necessary to have accurate values of the majority and minority electron mobilities in advanced semiconductor device simulation. Despite the importance of these quantities for device applications, such as bipolar transistors which are controlled by minority carrier flow in heavily doped regions, theoretical treatments are quite limited. There still remains a tendency in numerical simulation to assume that majority and minority mobilities are equal, although experiments have shown that majority and minority mobilities may differ by a factor of 3 in heavily doped Si [1][2][3][4].

Moreover, there is no theoretical model to date which explains the different mobility data for As- and P-doped Si for impurity concentrations higher than  $10^{18}$   $\text{cm}^{-3}$ . The difference between the electron mobility in As- and P-doped samples is up to 32 % at  $N_I = 4 \cdot 10^{21}$   $\text{cm}^{-3}$  [5]. Ignoring these phenomena can lead to incorrect interpretation of device data which strongly depend on doping concentration.

There were several attempts in the past to explain these different mobilities. Ralph et al. [6] introduced a central-cell scattering potential determined empirically using bound state energies of donors. Later, El-Ghanem and Ridley [7] employed a square-well impurity core potential. Bennett and Lowney investigated the majority and minority electron mobility in Si [8][9][10] and GaAs [11]. They introduced different scale factors in the interaction potential for majority and minority electrons.

The basis of our theoretical approach is the Thomas-Fermi (TF) theory [12][13]. This semi-classical treatment of the atom in the energy functional formulation yields the impurity charge density as a function of the atomic and electron numbers as well as a variational parameter which defines the size of the valence electron charge cloud. Knowing the charge density we obtain analytical expressions for the differential scattering cross section using the Born formalism up to second order to account for the charge sign of the impurity center.

## Charge Density of Ionized Impurities

The total valence charge density (in units of the electron charge  $e$ ) of an unscreened impurity atom with atomic number  $Z$  and electron number  $N$  in a solid is given by

$$\rho_{ion}(r) = Z\delta(r) - \rho_e(r) \quad (1)$$

$$N = \int \rho_e(\vec{r}) d^3r \quad (2)$$

The first term at the right hand side of Eq. (1) describes the nuclear charge density distribution concentrated in the origin. The second term,  $\rho_e(r)$  is the electron charge density of the impurity ion. There are numerous methods to calculate the electron charge density distribution. As we are interested in analytical solutions, we use the semi-classical TF model. Its basic idea is to treat the valence electrons as a degenerate Fermi gas of nonuniform, spherically symmetric electron density in a positively charged background at zero temperature. Under this assumption we get a local relation between the electron charge density and the Fermi energy. The total energy consists of the classical Coloumb potential energy of electron-electron  $E_{e-e}$  and electron-nucleus interactions  $E_{e-n}$ , and the kinetic energy  $E_k$ . Hence we define the total energy functional ( $\hbar = m = 1$ )

$$E_0 = E_k + E_{e-n} + \lambda E_{e-e} \quad (3)$$

$$E_k = c_k \int \rho_e(r)^{5/3} d^3r \quad (4)$$

$$E_{e-n} = -\frac{Z}{\epsilon_{Sc}} \int \frac{\rho_e(r)}{r} d^3r \quad (5)$$

$$E_{e-e} = \frac{1}{2\epsilon_{Sc}} \int \int \frac{\rho_e(r)\rho_e(r')}{|\vec{r} - \vec{r}'|} d^3r d^3r' \quad (6)$$

with  $c_k = \frac{3}{10}(3\pi^2)^{2/3}$  and a correlation parameter  $\lambda$ . We assume the electron charge density distribution to be of the form

$$\rho_e(r) = \frac{N\alpha^2 e^{-\alpha r}}{4\pi r} \quad (7)$$

Its Fourier transform

$$F(q) = \frac{N\alpha^2}{q^2 + \alpha^2} \quad (8)$$

is called the atomic form factor of the charge distribution. The variational parameter  $\alpha$  has to be determined by minimizing  $E_0$ . Calculating the first derivative of the total energy with

respect to the variational parameter  $\alpha$  and the electron number  $N$  we get two equations for  $\alpha$  and  $\lambda$ :

$$0 = \frac{\partial E}{\partial \alpha} \quad (9)$$

$$0 = \left. \frac{\partial E}{\partial N} \right|_{N=Z} \quad (10)$$

Condition Eq. (10) makes the chemical potential vanish for a neutral atom. Solving Eq. (9) and Eq. (10) with respect to  $\lambda$  and  $\alpha$  we obtain finally

$$\alpha = \frac{Z^{1/3}}{c_k^*} \frac{1 - 2 \left(\frac{Z}{N}\right)}{\frac{5}{3} - 4 \left(\frac{Z}{N}\right)^{1/3}} \quad (11)$$

with  $c_k^* = \frac{\Gamma(4/3)}{2} \left(\frac{3\pi}{4}\right)^{2/3} \left(\frac{3}{5}\right)^{7/3}$ .

## Scattering potential

We assume randomly located impurities of concentration  $N_I$ . With increasing  $N_I$  the average distance  $R$  between two impurities decreases such that scattering processes become important in which two or even more ions are involved simultaneously. To include multi-potential scattering to first order, we let pairs of impurities act as scattering centers. Since the impurity ion in a solid is screened by free carriers, the effective potential in momentum space for a pair of impurities can be written as

$$U(q) = V_0 \frac{Z - F(q)}{q^2 + \beta^2 G(\xi, \eta)} \left(1 + \exp(-i \vec{q} \cdot \vec{R})\right) \quad (12)$$

with  $V_0 = \frac{2m^*}{\hbar^2} \frac{e^2}{\epsilon_{sc}}$ . In Eq. (12) linear screening is assumed.  $\epsilon_{sc}$  is the dielectric constant of the semiconductor, and  $\beta$  the inverse Thomas-Fermi screening length which for an un-compensated semiconductor is given by

$$\beta^2 = \frac{4\pi n e^2}{\epsilon_{sc} k_B T} \frac{\mathcal{F}_{-1/2}(\eta)}{\mathcal{F}_{1/2}(\eta)}. \quad (13)$$

Here,  $k_B T$  is the thermal energy,  $q$  the momentum transfer, and  $n$  the free carrier concentration (no compensation is assumed). The screening function [14]

$$G(\xi, \eta) = \frac{1}{\mathcal{F}_{-1/2}(\eta)} \frac{1}{\xi \sqrt{\pi}} \int_0^\infty \frac{x}{1 + \exp(x^2 - \eta)} \ln \left| \frac{x + \xi}{x - \xi} \right| dx$$

$$\xi^2 = \frac{\hbar^2 q^2}{8m^* k_B T} \quad \eta = \frac{E_F - E_C}{k_B T} \quad (14)$$

represents the dielectric response of the conduction electrons to an external charge.  $\mathcal{F}_j$  denotes the Fermi integral of order  $j$  and  $\eta$  is the reduced Fermi energy. To avoid numerical integration in the Monte Carlo procedure we use a rational approximation for  $G$  of the form

$$G(\xi, \eta) \approx \frac{1 + a\xi^2 + b\xi^4}{1 + c\xi^2 + d\xi^4 + e\xi^6}. \quad (15)$$

The unknown coefficients  $a, b, c, d, e$  which have to be chosen such as to match the screening function at zero and for infinity [15].

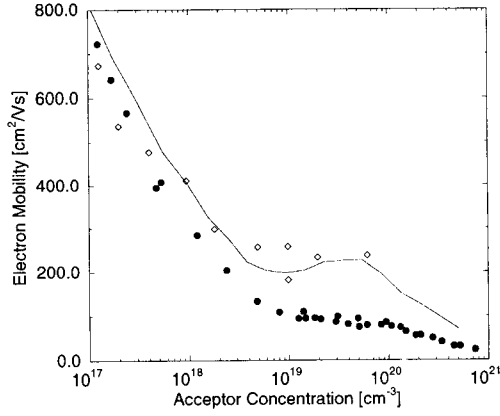


Figure 1: Minority electron mobility in B-doped Si. Simulation: solid line; experimental data from [4]: open diamonds; majority mobility data: filled circles [5]

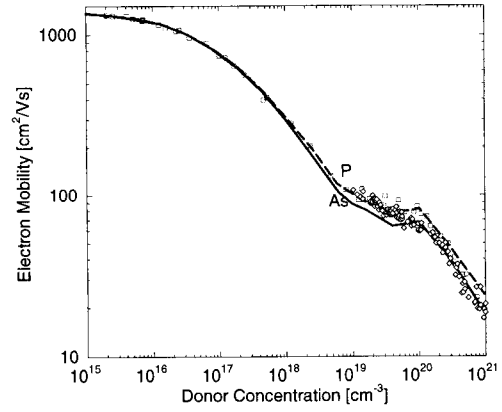


Figure 2: Majority electron mobility in P- and As-doped Si. Simulation: solid (As) and dashed lines (P); experimental data from [5]: open diamonds (As); open squares (P)

## Scattering Rate

With a given scattering amplitude  $f(q)$  the differential scattering cross section  $\sigma$  is defined as

$$\sigma(q) = \frac{(2\pi\hbar)^3}{m^*2v_g(k)} |f(q)|^2 \rho(E) \quad (16)$$

This expression is valid for arbitrary density of states  $\rho$  and group velocity  $v_g$ . Using the total cross section

$$\sigma_{tot}(k) = \frac{2\pi}{k^2} \int_0^{2k} \sigma(q) q dq, \quad (17)$$

the total scattering rate is given by

$$\lambda(k) = N_p v_g \sigma_{tot}(k) \quad (18)$$

where  $N_p = N_I/2$  is the density of impurity pairs.

## Results and Discussion

We present calculated mobilities for Si, GaAs, and InP at 300 K. The transport problem is solved by a Monte Carlo method. To avoid numerical integration for scattering rates in the Born approximation by calculating Eq. (17) and Eq. (18), we make use of an acceptance/rejection scheme[16].

All impurities were assumed to be ionized. In addition to ionized impurity scattering which is the main scattering process in heavily doped semiconductors, we took also into account acoustic intra-valley scattering, phonon inter-valley scattering, and electron-plasmon scattering. The latter effect lowers the mobility in  $p$ -type material significantly and is responsible for the dip in the minority mobility at about  $N_I = 10^{19} \text{ cm}^{-3}$ , which corresponds to the maximum strength of the electron-plasmon interaction[17]. The Pauli exclusion principle was included by means of a rejection technique assuming equilibrium Fermi-Dirac statistics for the final states.

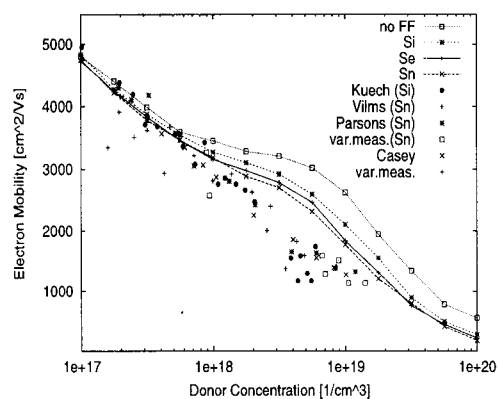


Figure 3: Majority electron mobility in GaAs for different donors

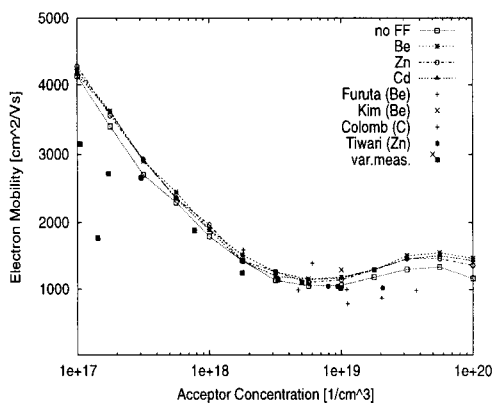


Figure 4: Minority electron mobility in GaAs for different acceptors

We have found that the momentum-dependent form factor strongly influences the scattering cross section with increasing doping concentrations, especially for minority electrons. Then larger scattering angles are becoming more probable such that the  $q$ -dependence of the atomic form factor cannot be neglected. The vanishing electron-plasmon interaction and the stronger repulsion are responsible for the increase of the minority electron mobility up to  $4 \cdot 10^{19} \text{ cm}^{-3}$  and the generally higher mobility in  $p$ -type Si (Fig. 1). The squared difference between  $Z$  and  $F(q)$  is higher compared to  $P$ -doped Si for the same energy because the effective charge of As-ions is larger than that in  $P$ -ions. Hence, the electron mobility is always lower in As-doped samples than in  $P$ -doped samples (Figs. 2). For  $n$ -GaAs our results confirm the lower mobility for donors with increasing atomic number  $Z$  above  $10^{18} \text{ cm}^{-3}$ . The mobility values may differ up to 20% at  $10^{19} \text{ cm}^{-3}$  for Si and Sn-doping, respectively (Fig. 3). In case of  $p$ -GaAs the influence of  $F(q)$  leads to a small increase of the mobility for acceptors. No significant dependence on the dopant species is observed over the whole concentration range (Fig. 4). In Fig. 5 and Fig. 6 the electron mobility in InP for different dopants is shown. These results are in agreement with the experiments of Anderson [18] who found no significant difference for various species. Unfortunately, the uncertainty and scattering of the available experimental data is of the same order of magnitude as the difference of the mobilities for various dopants. Hence, it is in general very difficult to evaluate the simulation results quantitatively.

## Conclusion

We have shown that consideration of the spatial charge distribution of the impurities is essential to explain the dopant-dependent electron mobility in heavily doped semiconductors. Hence, the failure of explaining different minority and majority electron mobilities for various dopant species in the past was due to neglecting the  $q$ -dependence of the atomic form factor which leads to different effective charges of the ionized dopants. Furthermore, in Si the two-ion correction is important over the whole doping range, whereas dispersive screening and the second Born correction are becoming important at  $N_I = 10^{18} \text{ cm}^{-3}$ . Due to the lack and inconsistency of experimental data for the minority electron mobility of all investigated semiconductors, it is difficult to compare our simulation results quantitatively for this particular case. It is hoped that the results outlined here will stimulate more experimental work to establish the different electron mobilities observed for various species of donors in  $n$ - and  $p$ -type semiconductors.

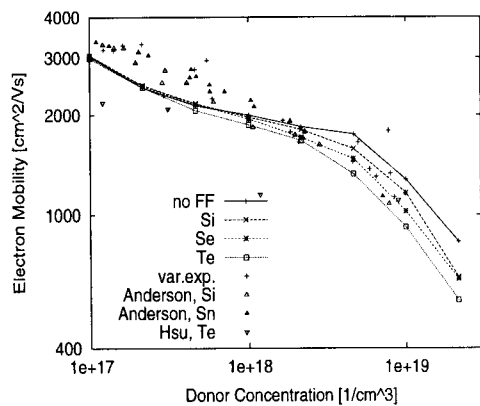


Figure 5: Majority electron mobility in InP for different donors

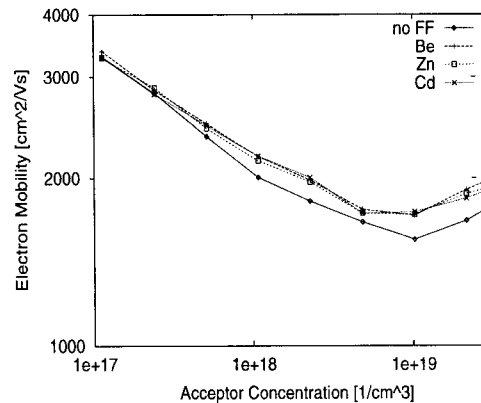


Figure 6: Minority electron mobility in InP for different acceptors

## References

- [1] J. Dziewior, *Appl.Phys.Lett.* **35**, 170 (1979).
- [2] I. Leu and A. Neugroschel, *IEEE Trans.Electron Devices* **40**, 1872 (1993).
- [3] A. Neugroschel, *IEEE Electron Device Lett.* **EDL-6**, 425 (1985).
- [4] S. Swirhun, D. Kane, and R. Swanson, in *Int.Electron Devices Meeting* (San Francisco, 1986), pp. 24–27.
- [5] G. Masetti, M. Severi, and S. Solmi, *IEEE Trans.Electron Devices* **ED-30**, 764 (1983).
- [6] H. Ralph, G. Simpson, and R. Elliot, *Physical Review* **11**, 2948 (1975).
- [7] H. El-Ghanem and B. Ridley, *J.Phys.C:Solid State Phys.* **13**, 2041 (1980).
- [8] H. Bennett, *Solid-State Electron.* **26**, 1157 (1983).
- [9] H. Bennett and J. Lowney, *J.Appl.Phys.* **71**, 2285 (1992).
- [10] H. Bennett and J. Lowney, in *Workshop on Numerical Modeling of Processes and Devices for Integrated Circuits NUPAD IV* (Seattle, 1992), pp. 123–128.
- [11] J. Lowney and H. Bennett, *J.Appl.Phys.* **69**, 7102 (1991).
- [12] E. Fermi, *Rend.Accad.Naz.Lincei* **6**, 602 (1927).
- [13] L. Thomas, *Proc.Camb.Philos.Soc.* **23**, 542 (1927).
- [14] D. Ferry, *Semiconductors* (Macmillan, New York, 1991).
- [15] H. Kosina and G. Kaiblinger-Grujin, *Solid-State Electron.* (1997), accepted for publication.
- [16] C. Jacoboni and P. Lugli, *The Monte Carlo Method for Semiconductor Device Simulation* (Springer, Wien-New York, 1989).
- [17] M. Fischetti, *Physical Review B* **44**, 5527 (1991).
- [18] D. Anderson, N. Apsley, P. Davies, and P. Giles, *J.Appl.Phys.* **58**, 3059 (1985).